Advanced Materials Research *Online: 2011-05-12*
ISSN: 1662-8985, Vols. 236-238, pp 829-834
doi:10.4028/www.scientific.net/AMR.236-238.829

Selective Methanation of CO over Mesoporous Nano Zirconian Supported Ni catalysts

Q. H. Liu[1, a], L. W. Liao[1, b], X. H. Zhou[1, c], and G. Q. Yin[1, d]

School of Chemistry and Chemical Engineering, ZhongKai university of agriculture and engineering, Guangzhou, china, 510225

[a]lqh2003@163.com, [b]liaolw@163.com, [c]cexinhuazhou@163.com, [d]yingq007@163.com

Keywords: Selective methantion, CO removal, Mesoporous nanocrystalline Zirconia, Ni/ZrO_2 catalysts.

Astract. Mesoporous nano zirconian was prepared by the self-assembly route using hexadecyltrimethyl ammonium bromide (CTAB) surfactant and employed as support for Nickel catalysts for selective methanation of CO. The CO methanation catalytic performance of the synthesized mesoporous nano zirconia-supported Ni-based catalysts was investigated, and the catalysts were charactered by TG/DSC, BET and XRD techniques. The results showed that, when the Ni loading was under 7.5 wt%, almost all the nickle species were in the form of nanoscale crystallites that finely distributed on the mosoporous nano zirconian surface. These well dispersive nickle species presented unique high activity and selectivity for CO methanation. For all the catalysts studied, the 7.5 wt%Ni/ZrO_2 catalyst was the most effective one, which showed a higher than 99% of CO conversion in the CO/CO_2 competitive methanation reactions over the temperature interval of 260~280°C, while the CO_2 conversion was held at the low level.

Introduction

Fuel cells have been considered as an effective generator system in recent years for its no emission of any pollutant gases [1]. The Proton-exchange Membrane Fuel Cells (PEM FC) are viewed as the most promising candidate for the power sources of small generators and vehicles [2]. PEM FC is fueled by hydrogen-rich gas mixtures usually generated by catalytic reforming of hydrocarbons, alcohols, methane or others followed by CO water gas shift reaction [3-5]. The obtained H2-rich gas inevitably contains 0.5~2 vol% CO, which poisons the PEM FC anode catalyst by strong adsorption of CO and must be removed to a level below 20 ppm [6-8]. Preferential CO oxidation (PROX) by adding air was considered to be one of promising method for the CO deep removal from the hydrogen-rich gas mixtures [9]. The Au-, Pt-, Ru-, Rh- and Cu-based supported catalyst were suggested to be the highly active and selective PROX catalytic system [10-12]. However, with the presently available catalysts, the undesired oxidation of hydrogen can not be avoided, and an accurate controlling system for the air injecting and the continuous monitoring of the inlet CO concentration were required, which causes additional complications of the PEM FC system. Furthermore, the nitrogen contained in the adding air caused unwanted dilution of the hydrogen-rich gas. CO removal from H_2-rich gas by selective methanation has been recently proved to be another effective strategy [13]. Compared to PROX, selective CO methanation has the benefit that no air additives to the H_2-rich gas stream, and the methane produced is inert to the PEM FC. The amount of hydrogen consumed by the CO methanation is small due to low CO content. The challenge of this method is the presence of relative high CO_2 concentration(20~25vol%). If the CO_2 methanation proceeded, considerable hydrogen losses may occur. Therefore, there is a need to develop a highly active and selective CO methanation catalyst that enables prevention of the CO_2 methanation. Recently, high-throughput combinatorial synthesis [14] and screening methods [15] were applied for CO and CO_2 methanation over zirconia and ceria supported noble and base metal catalyst in an attempt to discover new improved catalyst. It was reported that Ni-base and Ru-base catalysts were proved to be effective for selective CO methanation, and the performance of these catalysts could be somewhat varied by using various supports, promoters and preparation procedures [16]. It is considered that the Ni-based catalysts are less promising than the Ru-based catalysts, because they need long pretreatment in reducing atmosphere, possess pyrophoricity and rapidly lose activity in contact with air. Essential cost-efficiency is the main advantage of the Ni-based systems with respect to Ru-based ones. Consequently, it is important to develop precious-metal-free, highly active and selective catalysts for CO methanation in the presence of CO_2. Recently, we have suggested the nickel-zirconian based catalysts which demonstrate high activity and selectivity for CO methanation in reformate gas[17]. In the present work, a series nickle catalysts loading on mosoporous nano ZrO_2 were prepared and studied in the CO/CO_2 competitive methanation reactions. Catalytic performance of the catalysts for the selective methanation of CO was investagated and the catalysts were charactered by TG/DSC, BET and XRD.

Experimental

Catalyst preparation

The mosoporous nano ZrO_2 support employed in this study was prepared by the surfactant-assisted route. 1.0 g of CTAB dissolved in 20 ml of H_2O was added to a 10 ml 0.5 mol/L $ZrOCl_2 \cdot 8H_2O$ aqueous solution under vigorous stirring and was well mixed to ensure self-assembly. The pH of the mixed solution was adjusted to 9~10 by a 25% of ammonia solution, and the zirconium hydroxide sol-gel was formed. The obtained sol-gel precipitate was filtrated after aging for 48h at 90˚C and washed free of chlorine ions by deionized water and was dried at 110˚C for 12h. The dried solide was then calcined at 500℃ for 5h. The obtained sample was crushed into powders and used as the catalyst support with surface areas of 183 m^2/g, and the mean pore size was 6 nm.

The mosoporous nano ZrO_2 supported Ni catalysts were prepared by incipient wetness impregnation method. Prior to impregnation, the ZrO_2 was dried in an oven at 300°C for 2h. For the incipient wetness method, a defined volume of the solution containing the active metal salt was taken such that it was completely absorbed by the support material. By this method, the content of introduced nickel can be accurately controlled simply. After each impregnation, the wet sample was dried in air at room temperature for at least 12h, then dried at 110°C for 4h. After the final impregnation and drying, the sample was calcined at 500°C with a heating rate of 5°C/min for 3h. The obtained catalyst powders were pressed into pellets.

Catalyst characterization

The TG/SDC experiment was performed at a differential scanning calorimeter (DSC, TA SDT Q600). It was conducted at a heating rate of 10 K/min, with high-purity Ar (99.999%) as the protective gas. The real Ni and Ru loading of the ZrO_2 supported Ni catalysts was determined by inductively coupled plasma atomic emission spectrometry (ICP, IRIS ADVANTAGE. ER/S). The specific surface areas (S_{BET}) of the nano mosoporous zirconia support and of the catalysts were determined by BET method using a TriStar II 3020 apparatus. The XRD patterns were recorded using a Purkinje General XD-3 diffractometer using Cu Kα radiation with a 1.5406nm of incidence wavelength.

Catalytic reaction

The reaction was performed in a fixed-bed continuous-flow quartz reactor (i.d. 4 mm, catalyst bed length: 25 mm) at atmospheric pressure. In all experiments, 0.5 g of the catalyst (the particle size ranged 0.1-0.2 mm) was placed in the reactor. The temperature was measured by a chromel-alumel thermocouple in the middle of the catalyst bed. The experiments were performed with the following gas feed composition: 1 vol. % CO, 70 vol. % H_2, 3 vol. % H_2O, 23 vol. % CO_2, with N_2 as balance. Total feed flow rate was 3.2 cm^3s^{-1}(STP) to achieve a Weight Hour Space Velocity (WHSV) of 23,000 $cm^3g^{-1}h^{-1}$. To prevent the formation of volatile $Ni(CO)_x$, which is thermodynamically feasible at temperatures <150°C, the catalytic experiments were performed in the temperature internal of 180~320°C. Initially, the reactor with catalyst was heated to 180˚C in N_2 flow, then the reaction mixture was fed to the reactor upon continuous heating to 300°C; after that the reactor was cooled to 180°C and catalytic experiments were started. The inlet and outlet gas mixtures were analyzed on-line by a gas-chromatograph Agilent 6890 equipped with TDX-01 column and a thermal conductive detector (TCD). The detection limit of CO, CO_2, CH_4 and other gaseous hydrocarbons was ~1 ppm.

Results and discussion

Figure 1 shows the TG/DSC curves of the self-assembly zirconium hydroxide obtained during the preperation of the mesoporous nano ZrO_2 surppot by surfactant-assistant route. The TG curve was charactered by four segment of mass-loss. The mass-loss at lower 150˚C was due to the volatilization of the dissociated water, and the mass-loss between 150˚C and 230˚C was caused by the removal of crystal water of the zirconium hydroxide. The mass-loss of the decomposition of CTAB by heat occurred at the temperature range of 230~380°C, for which the mesoporous of the nano ZrO_2 were formed. The decomposition of CTAB could be further explained by the exothermic peak at 322°C on the DSC curve. The mass-loss from 380°C to 480°C was attributed to the tranformation of tetragonal zirconia to monoclinic zirconia [18], which corresponding to a distinct exothermic peak at 438°C on the DSC curve. When the temperature was increased to higher than 490℃, no evident mass-loss was found on the TG curve, indicating that the mesoporous nano ZrO_2 had been in the thermal stable state.

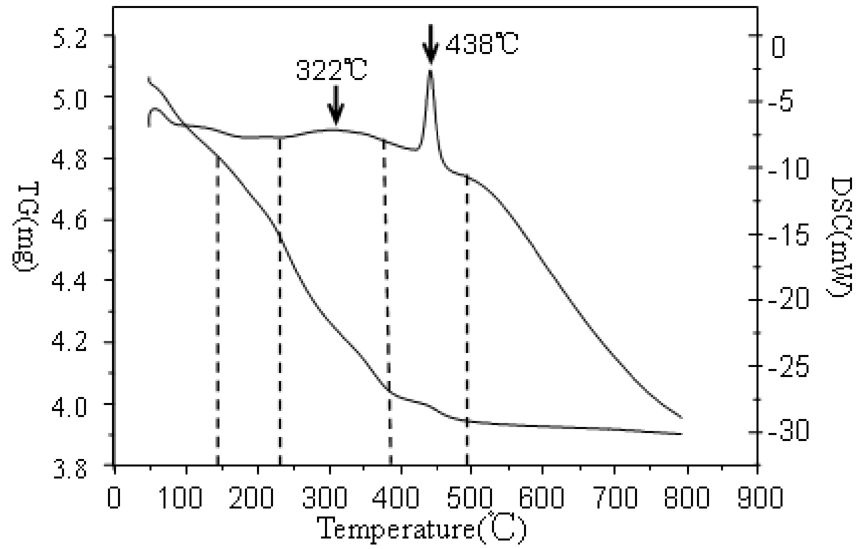

Figure1. TG/DSC curves of the self-assembly zirconium hydroxide

Table 1 presents real Ni loading, calcination temperature and specific surface areas of the mesoporous ZrO_2 and the as-synthesized Ni/ZrO_2 catalysts. The real Ni loading was close to the calculated one for all samples. S_{BET} monotonically decreased from 183m^2/g (for ZrO_2 support) to 64 m^2/g (for 20Ni/ZrO_2) with increasing Ni loading.This trend is typical for supported metal catalyst and is attributed to the blocking of ZrO_2 pores by Ni particles and by increasing number and size of the low-surface Ni particles [19].

Table 1 The S_{BET} of the catalysts employed in the present study

sample	Ni loading(wt.%)	Calcination Temperature (℃)	S_{BET}(m^2g^{-1})
ZrO_2	-	500	183
$2Ni/ZrO_2$	1.9	500	176
$4Ni/ZrO_2$	3.7	500	139
$8Ni/ZrO_2$	7.5	500	93
$15Ni/ZrO_2$	13.7	500	76
$20Ni/ZrO_2$	18.6	500	64

Figure 2 presents the XRD patterns of the mesoporous nano ZrO_2 and the Ni/ZrO_2 catalysts with various Ni loading. It was shown that the XRD patterns of the Ni/ZrO_2 catalyst with Ni loadings from 1.9 wt% to 7.5 wt% were the same as that of the ZrO_2 support, illustrating neither nickel oxide, nor metallic nickel peaks. This phenomenon was attributable in large part to the nickel species in these catalysts existed in the form of finely dispersed on the mesoporous nano ZrO_2 surface[17]. As the Ni content increased to higher($15Ni/ZrO_2$, $20Ni/ZrO_2$ catalysts), the peaks corresponding to nickel oxide appeared in the XRD patterns, indicating that at least part of Ni species in these catalysts conglomerated to form large oxide bulk. However, the Ni loading determined from the XRD data for these catalysts was considerably lower than the real Ni loading. This fact suggests that considerable parts of Ni species in the catalysts were not detected by XRD because most of them were well dispersed, in the form of nanoscale crystallites below the XRD detectable limit, on the mesoporous nano ZrO_2 surface. Below we consider the Ni/ZrO_2 catalysts' performance for selective CO methanation in the reformate gas.

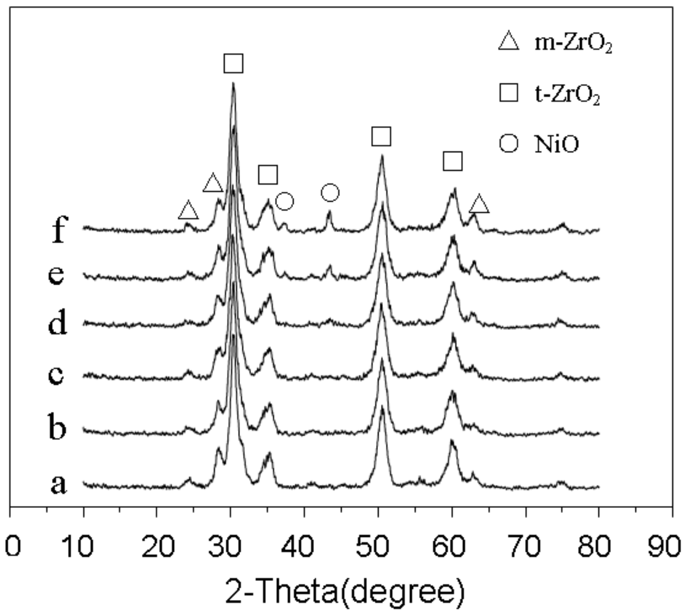

Figure 2. XRD patterns of the mesoporous nano ZrO_2 (a) and the as-synthesized $2Ni/ZrO_2$ (b), $4Ni/ZrO_2$ (b), $8Ni/ZrO_2$ (c), $15Ni/ZrO_2$ (d), and $20Ni/ZrO_2$ (e) catalysts.

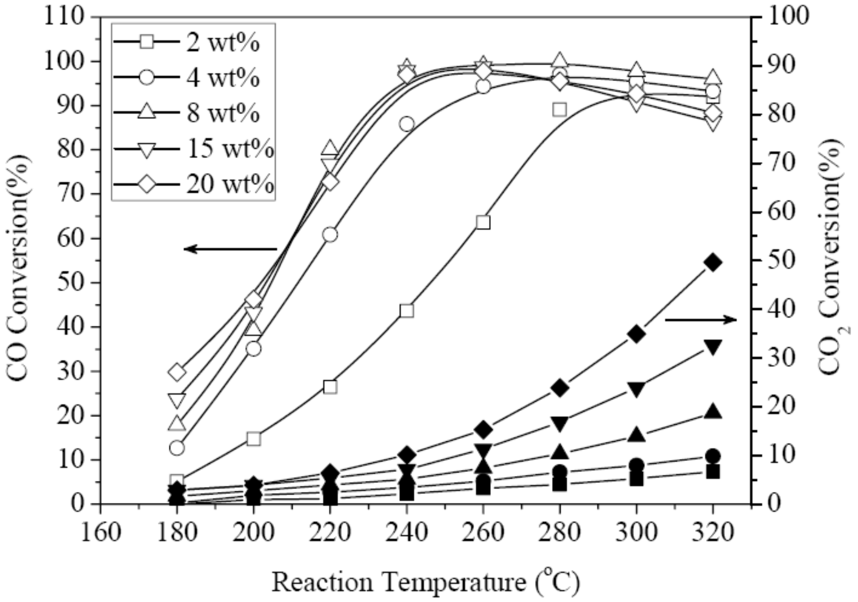

Figure 3. Effect of Ni loading of the Ni/ZrO_2 catalyst on the CO conversion(open) and the CO_2 conversion (solid). (□) $2Ni/ZrO_2$, (○) $4Ni/ZrO_2$, (△) $8Ni/ZrO_2$, (▽)$15Ni/ZrO_2$, (◇)$20Ni/ZrO_2$

Figure 3 presents the temperature dependencies of the CO concentration and CO_2 conversion at selective CO methanation over $2Ni/ZrO_2$, $4Ni/ZrO_2$, $8Ni/ZrO_2$ $15Ni/ZrO_2$ and $20Ni/ZrO_2$ catalysts. For all Ni/ZrO_2 catalysts, the CO conversion first dramaticly increased, reached a minimum, and then decreased with the increasing temperature. They are typical for the reaction of selective CO methanation. As the Ni loading in the catalysts increased, the temperature dependencies of the CO methnation rection shifted to the lower temperature region. The most profound shift was observed from the $2Ni/ZrO_2$ catalyst to $4Ni/ZrO_2$ catalyst. The high-loaded nickel catalysts ($15Ni/ZrO_2$ and $20/NiZrO_2$) demonstrated similar temperature dependencies of the CO methanation. In the temperature interval of 180~240°C, CO methanation preferentially proceeded on all the catalysts and high selectivity of CO methanation was observed. At higher temperature, the selectivity was decreased and, probably, RWGS to proceed in parallel with the CO methanation [20, 21]. As for the reaction of CO_2 methanation over Ni/ZrO_2 catalysts, noticeably occurred at temperatures above 220℃. With the temperature increased from 220 to 320℃, the CO_2 conversion increased rapidly and the selectivity of the CO methanation decreased for all catalysts. While the Ni loading increasing, the CO_2 conversion significantly increased, this illuminated that the activity of the Ni/ZrO_2 catalysts for the reaction of CO_2 methanation increases with increasing Ni loading in this order:

$$2Ni/ZrO_2 < 4Ni/ZrO_2 < 8Ni/ZrO_2 < 15Ni/ZrO_2 < 20Ni/ZrO_2$$

whereas the selectivity with respect to CO methanation increases in reverse order. The increase of the supported nickel surface area (S_{Ni}) with increasing nickel loading, and the presence of small and large NiO particles in the catalysts represent probable reasons for these observations. Likely, the supported nickel surface area increases most drastically in order $2Ni/ZrO_2 < 8Ni/ZrO_2$. In these catalysts nickel exists as small crystallites distributed uniformly over zirconia surface. With loading up, the number of these small crystallites obviously increases that leads to the increase of S_{Ni} and catalytic activity. Nickel in the high-loaded catalysts($15Ni/ZrO_2$, $20Ni/ZrO_2$) exists as both small and large crystallites. The high activity and lower selectivity for CO methanation over the high-loaded catalysts as compared to the low-loaded ones can be explained by that the CO_2 methanation reaction occurs predominantly on the large nickel particles and the CO mehtanation was took place large partly on the dispersive small nickle active sites[16]. As figure 3 shows, for all the catalysts studied, the 7.5 wt% Ni/ZrO_2(8 Ni/ZrO_2) is the most effective for selective CO methanation. which presents the higher than 99% of CO conversion in the temperature window of 260~280℃, while the CO_2 conversion was held relative low.

Conclusions

Selective CO methanation in the reformed gas was performed over the 1.9~18.6 wt.% Ni based catalysts loading on the mesoporous nano ZrO_2 support synthesized by the CTAB surfactant-assistant route. All catalysts studied show high activity for CO methanation. The selectivity of the catalysts was significantly affected by the nickle loading Among all the catalysts prepared, the 7.5 wt %Ni/ZrO_2 catalyst is the most effective for selective mehthanation of CO, which is largely comprised of nanoscale nickle crystallites that finely distributed on the mesoporous nano zirconia surface. This catalyst presented a higher than 99% CO converions in the CO/CO_2 competitive methanation reactions at the temperature range of 260~280˚C, while the CO_2 conversion was all along kept at the low level.

Acknowledgements

This work was financially supported by the Natural Science Foundation of Zhongkai University of Agriculture and Engineering (G3100026).

References

[1] P. Costamagna, S. Srinivasan. J. power and sources. vol. 102 (2001), p. 253

[2] S. Q. Song, P. Tsiakaras. Appl. Catal. B. vol. 63 (2006), p. 187

[3] Q. B. Liu, H. Hong, J. L. Yuan, Jin, G. C. Hong, X.Rui. Appl. Energy. vol. 86 (2009), p. 155

[4] F. V. Stefan Rabe. Appl. Catal. B. vol. 84 (2008), p. 827

[5] T. J. Huang, M. C. Huang. Chem. Eng. J. vol. 145 (2008), p. 149

[6] S. Gamburzev, A. J. Appleby. J. Power Sources. vol. 107 (2002), p. 5

[7] L. T. David, Z. I. önsan. catal. reviews. vol. 43 (2001), p. 31

[8] C. P. Huang, R. C. Jiang, M. Elbaccouch, N. Muradov, J. M. Fenton. J. Power Sources. vol. 162 (2006),p. 563

[9] D. L. Trimm. Appl. Catal. A. vol. 296 (2005), p. 1

[10] H. B. Zou, X. F. Dong, W. M. Lin. Appl. Surf. Sci.. vol. 253 (2006), p. 2893

[11] X. R. Chen, H. B. Zou, S. Z. Chen, W. M. Lin. J. Natural Gas Chemistry. vol. 16 (2007), p. 409

[12] Y. Q. Huang, A. Q. Wang, L. Li, et al. J. Catal. vol. 255(2008), p 144

[13] R. A. Dagle, Y. Wang, G. Xia, J. J.Strohm, J.Holladay, D. R. Palo. Appl. Catal A. vol. 326 (2007), p. 213

[14] M. Krämer, M. Duisberg, K. Stöwe, et al. J. Catal. vol. 251 (2007), p. 410

[15] K. Yaccato, C. Ray, H. Alfred, L. Andreas, S. Peter, F. V. J.Anthony, T. Howard, W. Henry, K. G. Robert, B. Chris. Appl. Catal. A. vol. 296 (2005), p. 30

[16] S. Takenaka, T. Shimizu, K. Otsuka. International J. Hydrogen Energy. vol. 29 (2004), p. 1065

[17] Q. H. Liu, X. F. Dong, X. M. Mo, W. M. Lin. J. Natural Gas Chemistry. vol. 17 (2008), p. 268

[18] J. M. Criado, M. González, M. J. Diánez, L.A. Pérez-Maqueda, J. Málek. J. Phys. and Chem. Solids. vol. 68 (2007), p. 824

[19] B. Kester, E. Zagli, L. Falconer. Appl. Catal. vol. 22(1986), p. 311

[20] S. B.Marcelo, I. S Elisabete, M. A Elisabete, A. T.Edson. J. Power Sources. vol. 145 (2005), p. 50

[21] S. H. Kim, S. W. Nam, T. H. Lim, H. I. Lee. Appl. Catal. B. vol. 81 (2008), p. 97